Self-consistent simulations of beam-beam interaction in future e^+e^- circular colliders including beamstrahlung and longitudinal coupling impedance

Yuan Zhang,[*,†] Na Wang, Chuntao Lin,[‡] Dou Wang, and Chenghui Yu[§,‖]
Key Laboratory of Particle Acceleration Physics and Technology, Institute of High Energy Physics, Chinese Academy of Sciences, 19(B) Yuquan Road, Beijing 100049, China

Kazuhito Ohmi
KEK, Tsukuba, Ibaraki 305-0801, Japan

Mikhail Zobov
INFN-LNF, Frascati, 00044 Roma, Italy

(Received 14 August 2020; accepted 30 September 2020; published 15 October 2020)

For the past generation e^+e^- storage ring colliders, we usually used natural bunch length or its impedance lengthened value in beam-beam simulations instead of considering the impedance directly. In the future colliders, such as FCC-ee and CEPC, the beam-beam interaction becomes essentially three dimensional. In order to increase the luminosity, the future accelerators will collide very intense beams of high energy with low emittances and small beta functions at the collision points exploiting the crab waist collision scheme with a large Piwinski angle. For these extreme parameters several new effects become important for the collider performance such as beamstrahlung, coherent X-Z instability, 3D flip-flop so that the longitudinal beam dynamics should be also treated in a self-consistent manner. In this paper we describe the numerical code for the self-consistent 3D beam-beam simulations including beamstrahlung and the longitudinal beam coupling impedance and study interplay of different effects arising in beam-beam collisions of the future colliders.

DOI: 10.1103/PhysRevAccelBeams.23.104402

I. INTRODUCTION

The beam-beam interaction in storage rings has been studied since 1960 (see [1], as an example). A lot of fruitful work has been done since then in order to improve the collider performance. Different techniques and collision schemes have been proposed to increase their luminosity [2]. For the last generation of electron-positron factories, a collision of intense multibunch beams was one of the main ingredients to increase their luminosity. The crossing angle between colliding bunches was necessary to alleviate the parasitic beam-beam interaction and the operations with the horizontal crossing angle were successful at the lepton particle factories such as KEKB [3], DAΦNE [4] and BEPCII [5]. For these machines the Piwinski angle $\Phi = (\sigma_z/\sigma_x)\tan(\theta/2)$ was chosen to be relatively modest, of the order of 0.5 (1.7 in DAΦNE only after 2007), to avoid an excessive geometric luminosity reduction and to diminish the strength of synchrobetatron resonances arising from the beam-beam interaction with the crossing angle.

However, it has been noticed by several authors that a large Piwinski angle can help to increase the luminosity [6–8]. The most important feature is that the large Piwinski angle allows squeezing the vertical beta function β_y at the interaction point (IP) down to the scale σ_x/θ [9]. In addition to the possibility of having very small beam sizes at IP, such a collision scheme also reduces substantially the horizontal beam-beam tune shift [10] and also helps suppressing the vertical synchro-betatron resonances [11].

The further luminosity increase can be reached applying the crab waist (CW) collisions scheme by installing dedicated sextupoles in the interaction region before and after the interaction point and by imposing special conditions on the betatron functions at the sextupole locations and on the phase advance between the sextupoles and IP [9]. The crab waist collision scheme eliminates the beam-beam resonances arising (in collision without CW) due to the vertical motion modulation by the horizontal betatron oscillations [12,13].

[*] zhangy@ihep.ac.cn
[†] Also at University of Chinese Academy of Science.
[‡] Also at University of Chinese Academy of Science.
[§] yuch@ihep.ac.cn
[‖] Also at University of Chinese Academy of Science.

For the first time a combination of the large Piwinski angle and the crab waist collisions has been successfully applied in DAΦNE [14] and since recently it is exploited at SuperKEKB giving very promising results [15].

The first electron-positron Higgs factory based on circular storage rings was proposed already several months before the official announcement of the Higgs boson discovery [16]. The proposal has evolved, first passing to DLEP, the e^+e^- collider having the double LHC circumference, and then to TLEP Triple LEP hosted in a 80 to 100 km tunnel [17]. At present the two 100 km long electron-positron colliders, FCC-ee in Europe [18] and CEPC in China [19], are under study as possible future accelerators to explore the properties of the Higgs, W and Z bosons as well as the top quark production thresholds with unprecedented precision.

In order to reach the high luminosity, both colliders are expected to use the crab waist collision scheme with a large Piwinski angle relying on collisions of very intense multi-bunch beams of high energy with low emittances and small betatron functions at the interaction point. For these extreme parameters several new effects become important for the collider performance such as beamstrahlung [20], coherent X-Z instability [21] and 3D flip-flop [22]. Beamstrahlung is the synchrotron radiation induced by beam-beam force. The X-Z instability, which appears in the correlated head-tail motion of two colliding beams, is a novel coherent beam-beam instability in collisions with a large crossing angle. The beam dynamics becomes essentially three dimensional and the longitudinal motion can no longer be considered as frozen. Moreover, interplay of different beam dynamics effects becomes very much important for the choice of the collider parameters and their optimization.

In both future lepton colliders beamstrahlung leads to a substantial energy spread growth and bunch elongation in beam-beam collisions [18,19]. On the other hand, the bunch electromagnetic interaction with surrounding accelerator equipments, described in terms of beam coupling impedance, also results in a notable bunch lengthening [19,23,24]. In addition, the impedance is responsible of the synchrotron tune reduction and synchrotron tune spread increase [23]. Beyond the threshold of the microwave instability that is driven by the coupling impedance the energy spread starts growing and the internal bunch oscillations can take place. In the conceptual design reports of the future colliders [18,19] these effects, beamstrahlung and the impedance related effects, have been studied separately.

Recently the first semianalytical model has been developed to study interplay of these effects [25]. In particular, it has been shown that the bunch becomes somewhat longer, the energy spread slightly reduces and the synchrotron frequency reduction gets smaller. However, the model assumes that the bunch current stays below the microwave instability threshold and the beam dynamics is not affected by the beam-beam instabilities.

The real situation is even more complicated since the newly discovered coherent beam-beam instability arising in collisions with a large crossing angle [21] couples the transverse and longitudinal planes of motions (the X-Z instability). In turn, the beamstrahlung and the beam coupling impedance will affect the coherent instability and the 3D flip-flop respectively. The performance of the colliders and the choice of the good working points will also be affected by the combined effects. Thus fully 3D self-consistent simulations of beam-beam interaction including beamstrahlung and the beam impedance are urgently required for the collider parameter optimization and interplay of the different effects is to be studied in detail.

In Sec. II we describe the 3D numerical code IBB that has been developed to perform such studies, while Sec. III discusses the principal results of the numerical simulations. Here we mainly focus on studies of the X-Z instability and its impact on the future collider performance. In subsection A of Sec. III we show the self-consistent results for CEPC including both the impedance and beamstrahlung effects. In subsections B and C these effects are studied separately in order to understand the results obtained in subsection A. Finally in subsection D of Sec. III we consider the real scenario for future colliders including the bootstrapping injection in collision. The summary of the results is given in Sec. IV.

II. MODEL OF SIMULATION

The simulation code IBB used in the paper has been developed for the design and optimization of BEPCII [26], and has been extended to support large Piwinski angle collision, beamstrahlung effect, multiple bunches/multiple IPs. In the code, the one turn map is the following: (1) beam-beam interaction at IP, where beamstrahlung may be considered. (2) linear map considering synchrotron radiation effect (damping + fluctuation) [27] during the transportation through the arc. (3) longitudinal wakefield of the whole ring lumped at IP before collision.

A. Beam-beam interaction

Since the beam-beam force is very nonlinear, the quantitative study requires comprehensive numerical simulations. In the early stage, the rigid bunch model has been used to study the coherent mode [28]. The weak-strong simulation method has been generally used to design colliders [29–32] based on the prediction of luminosity and the lifetime estimation due to the formation of non-Gaussian halos [33,34]. With weak-strong model, wide-range parameters scan is possible even nowadays.

Due to the hourglass effect, the geometric luminosity reduction and the transverse beam-beam blowup depend on the finite bunch length. In order to take this effect into account, the colliding bunches are sliced in the longitudinal direction. In order to speed up the convergence of the slice number, the potential interpolation method is used [35].

The Lorentz boost map [6] is used to consider the horizontal crossing angle. The bunch slice number is usually about ten times the Piwinski angle.

In order to calculate the beam-beam potential, we directly solve the Poisson equation by applying the particle-in-cell (PIC) method. The fast Fourier transform (FFT) method using shifted integrated Green function [36] is adopted, which is very helpful to handle the separated slice-by-slice collision in large Piwinski angle collision.

The strong-strong simulations of the beam-beam interaction with a large Piwinski angle are very time consuming [37]. So we prefer to use the synchro-beam mapping method [38] to model the slice-slice collision, where the Gaussian approximation is used. In addition, we update the slice transverse RMS size in each slice-slice collision. The Gaussian strong-strong method used in the paper is about one order of magnitude faster than the PIC strong-strong method.

Beamstrahlung is the synchrotron radiation induced by beam-beam force. The energy of beamstrahlung photons emitted during collision is much higher than that from the normal bending magnets. The random emitted photon energy is modelled using bending magnet radiation with the Monte-Carlo method [39].

B. Longitudinal wakefield

The longitudinal wake potential is calculated self-consistently and taken into account directly before IP in each turn. The wake potential $V(t)$ is defined as the energy loss per unit charge for a particle. The voltage spectrum could be obtained by multiplying the current spectrum by the impedance

$$\tilde{V}(\omega) = -\tilde{I}(\omega) Z_{\parallel}(\omega). \tag{1}$$

where the longitudinal impedance $Z_{\parallel}(\omega)$ is defined as the Fourier transform of the wake function $W_{\parallel}(z = -ct)$, i.e., the Green function of a point charge [40]:

$$Z_{\parallel}(\omega) = \int_{-\infty}^{\infty} \frac{dz}{c} e^{-i\omega z/c} W_{\parallel}(z). \tag{2}$$

The current could be written as an integral over a frequency spectrum:

$$I(t) = \int_{-\infty}^{\infty} \frac{d\omega}{2\pi} e^{-i\omega t} \tilde{I}(\omega). \tag{3}$$

The effective rf voltage reduction due to the longitudinal wakefields results in the bunch lengthening in the case of the potential well distortion (PWD). The same voltage reduction results also in the synchrotron frequency reduction [41]. A semianalytical model has been developed recently to study the combined effect of beamstrahlung due to collision and coupling impedance in the future lepton colliders [25]. In the following we will show the impact of the coupling impedance on the X-Z instability. It could be expected that the stable areas in horizontal tune space would shift because of the synchrotron frequency reduction induced by the impedance.

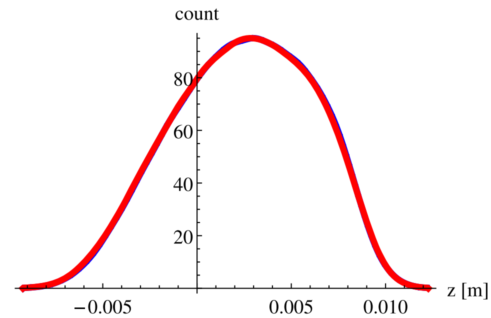

FIG. 1. Longitudinal distribution (collision off) obtained using ELEGANT and IBB considering the CEPC longitudinal impedance model.

C. Cross-check

The beam-beam interaction code IBB has been developed since about 2005 [26]. It has been checked in BEPCII, and the luminosity difference is about 10%–20% [42]. It has further been crosschecked with another strong-strong code BBSS [43], considering beamstrahlung effect [44]. The consideration of longitudinal impedance is the new feature of IBB, where the wake potential is computed by frequency domain multiplication of impedance and beam spectrum. Fig. 1 shows the longitudinal bunch distribution simulated by ELEGANT [45] and IBB, where collision is turned off and parameters in Table I are used except bunch population ($N = 3.12 \times 10^{10}$). The result of the two codes coincides very well. Here the impedance of CEPC has been used in the simulation. The bunch lengthening and energy spread is also checked using FCC-ee parameters and resistive wall data without collision [46], and the result agrees well with that presented in [23].

CEPC impedance model, which includes both resistive wall and the dominant geometrical impedances, has been used in the following studies. More detailed descriptions of the impedance can be found in [47]. The real and imaginary part of the longitudinal impedance are shown in Fig 2. The geometrical impedances are calculated with codes CST [48] and ABCI [49], while the resistive wall impedance is calculated with the theoretical formula [50].

III. SIMULATION RESULT

The parameters used in this paper are listed in Table I. Note that with respect to CEPC CDR data [19], the horizontal beta

TABLE I. Machine parameters[a].

Energy E (GeV)	45.5
Bunch population N (10^{10})	8
Emittance $\epsilon_{x/y}$ (nm/pm)	0.18/1.6
Beta at IP $\beta^*_{x/y}$ (m/mm)	0.15/1.0
Synchrotron tune ν_s	0.014
Damping time (turn) (X/Y/Z)	5055.6/5055.6/2527.8
Bunch length σ_z (mm) (SR/BS/BS + ZL)	2.42/7.20/7.39
Energy spread σ_p (10^{-4}) (SR/BS/BS + ZL)	3.80/11.3/10.5
Piwinski angle (SR/BS/BS + ZL)	7.7/22.9/23.3
Beam-beam ξ_x (SR/BS/BS + ZL)	0.037/0.0042/0.0041
Beam-beam ξ_y (SR/BS/BS + ZL)	0.25/0.084/0.082

[a]SR: Only considering synchrotron radiation in the ring and without collision. BS: Collision with beamstrahlung effect is also considered. BS + ZL: Both beamstrahlung and longitudinal coupling impedance are also considered.

function at IP has been reduced from 0.2 m to 0.15 m in order to mitigate the X-Z instability. Since there are two symmetrical IPs in the rings, the parameters listed here are for half ring. We do not consider the multiple IP effect in the paper. With large Piwinski angle, the good region of tune footprint is reduced to the area bounded by the main coupling resonance $Q_x - Q_y = n$, sextupole resonance $Q_x + 2Q_y = n$, and half-integer resonance $2Q_x = 1$ with its synchrotron satellites [22]. Since the instability we are interested in is not sensitive to the vertical tune, the fractional part of vertical tune is kept constant at 0.61.

A. Self-consistent simulation

In this section we compare two scenarios, with and without longitudinal impedance [47]. In both cases the beamstrahlung effect is turned on. The calculated equilibrium bunch length is 7.39/7.20 mm with and without impedance respectively. The equilibrium energy spread is $1.05/1.13 \times 10^{-3}$ with and without impedance respectively. It could be noticed that the bunch length is longer, while energy spread is smaller when the longitudinal wakefield is considered, even if the difference is only about a few percent. When we consider wakefield self-consistently, it is very natural to expect that the bunch will be longer than that only with beamstrahlung. Since the bending radius due to beam-beam force in large Piwinski angle collision is proportional to $\sigma_x\sigma_z$ [51] and the effective length of the overlap area is proportional to σ_x/θ [9], the beamstrahlung effect is weakened due to the longer bunch length induced by wakefield. Then it could be concluded that the equilibrium energy spread considering wakefield is smaller.

The horizontal tune has been scanned to check the tune width of stable collision. Since the typical phenomenon of the X-Z coherent beam-beam effects is the growth of the horizontal emittance, we use the growth rate of the horizontal beam-size as the figure of merit of the instability. Figure 3 shows the collision stability versus horizontal tune with and without longitudinal impedance. There exist some clear changes when the impedance is considered: (1) the shift of stable tune area; (2) the squeeze of stable tune area; (3) decrease of growth rate. It seems that the width of stable working point is too narrow for the considered configurations. It is necessary to re-optimize the machine parameters and to reduce further the impedance budget. More details on the machine parameter optimization are discussed in [19,22]. The effect of impedance is studied by simulation in Sec. III C.

Normally a machine is designed to run below single bunch microwave instability threshold. In our case, the threshold bunch population is only about 6×10^{10}, which is lower than the design bunch population 8×10^{10} [47].

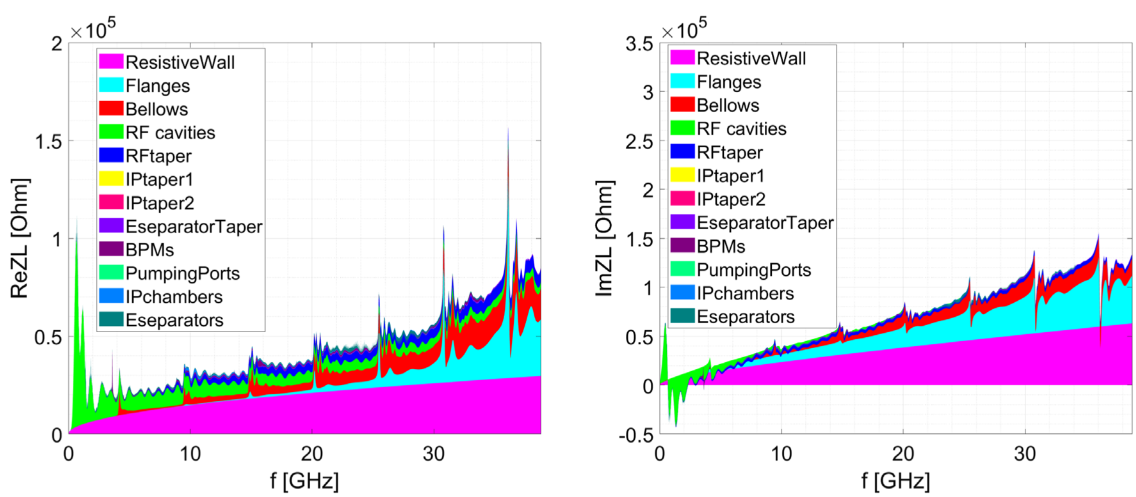

FIG. 2. The longitudinal impedance of CEPC.

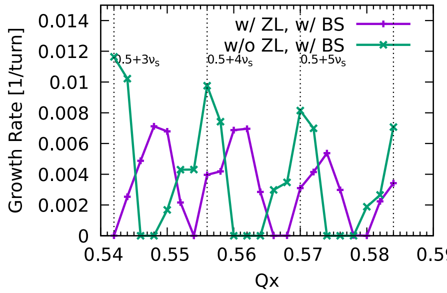

FIG. 3. The horizontal beam size growth rate versus horizontal tune with and without longitudinal coupling impedance (ZL). Beamstrahlung (BS) effect is turned on.

Fig. 4 shows the evolution of RMS energy spread with and without collision considering longitudinal wakefield at design bunch population. The violent instability due to impedance alone is damped by the beam-beam interaction with beamstrahlung effect, where the bunch length/energy spread is increased by a factor of 3. The microwave instability would not be a concern in collision with the help of beamstrahlung.

B. Beamstrahlung effect

In order to study the influence of the beamstrahlung effect alone on the beam-beam instability, the impedance is totally neglected here. To clarify possible beam dynamics effects of the beamstrahlung, we turn it off and on and scan the horizontal tune to check the difference. The equilibrium bunch length and energy spread without beamstrahlung is kept same as that with beamstrahlung in collision by tuning the natural equilibrium value (only considering synchrotron radiation) of the ring, where the longitudinal damping time does not change. Same bunch length and energy spread ensure the same beam-beam parameter with and without beamstrahlung in collision.

Figure 5 shows the difference of the collision stability with and without beamstrahlung. The left bound of one stable tune area is not sensitive to the model, with or without beamstrahlung, and the distance to the nearest resonance line is about 0.004, the value of beam-beam ξ_x. But the right bound would shift about 0.004, the value of

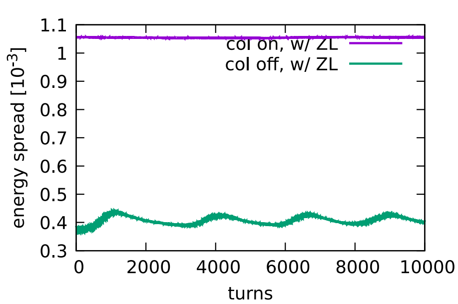

FIG. 4. Evolution of RMS energy spread considering longitudinal wakefield (ZL) with and without collision. Beamstrahlung effect is turned on during collision.

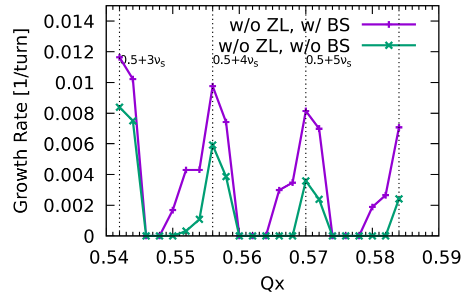

FIG. 5. The horizontal beam size growth rate versus horizontal tune with and without beamstrahlung effect (BS). The stable equilibrium bunch length and energy spread is same between the two cases, where $\sigma_{z,\mathrm{SR}}$ and $\sigma_{p,\mathrm{SR}}$ are tuned in latter case.

ξ_x, when we turn on the beamstrahlung effect. That is to say, the width of stable collision tune area would be reduced by about ξ_x. It has already been pointed out in [22] that ξ_x/ν_s should be small enough, and here this condition is proven again.

It is clear that the collision without beamstrahlung is more stable for same final equilibrium bunch length and energy spread. This could be explained by the fact that radiation coming from horizontal beam-beam force depends on the horizontal coordinate, which enhances the X-Z instability. According to the analysis of [51], the bending radii in horizontal and vertical plane during collision is similar.

C. Longitudinal wakefield

In order to study the influence of longitudinal coupling impedance on the beam-beam instability, the beamstrahlung effect is switched off here. The equilibrium bunch length and energy spread during collision are kept same with and without longitudinal coupling impedance, which ensure the same beam-beam parameter. This could help to evidence the effect of the wakefield alone. The value of equilibrium bunch length and energy spread here is tuned to be equal to that with both beamstrahlung and longitudinal coupling impedance by changing the natural synchrotron radiation equilibrium ones.

The horizontal tune is scanned with and without longitudinal coupling impedance, which is shown in Fig. 6. The effect is similar to that we have found before: (1) stable tune area is shifted; (2) stable tune area is squeezed; (3) instability growth rate is lower. The incoherent synchrotron tune shift and spread with and without the longitudinal wakefield is shown in Fig. 7. As we can see analyzing Fig. 6 and Fig. 7, the stable areas horizontal tune shift can be explained by the impedance related synchrotron tune shift. For example, the shift of the coherent beam-beam resonance from $Q_x = 0.57$ to 0.56 shown in Fig. 6 corresponds to the longitudinal tune shift of about 0.002 (see Fig. 7) multiplied by 5 that is the resonance number. In our opinion, the larger tune spread helps to reduce the growth rate of the beam-beam instability presumably due to the

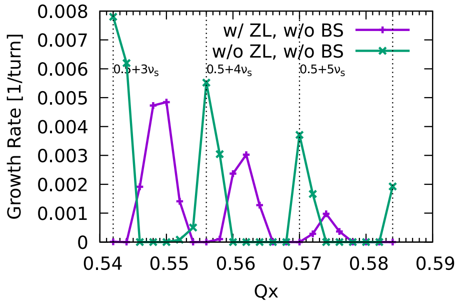

FIG. 6. The horizontal beam size growth rate versus horizontal tune with and without longitudinal coupling impedance (ZL), where beamstrahlung (BS) effect is turned off in both cases. The stable equilibrium bunch length and energy spread is same between the two cases, where $\sigma_{z,\mathrm{SR}}$ and $\sigma_{p,\mathrm{SR}}$ are tuned in latter case.

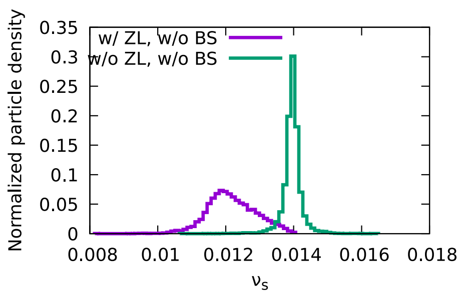

FIG. 7. Incoherent synchrotron tune with and without longitudinal wake (ZL), where beamstrahlung (BS) effect is turned off. The stable equilibrium bunch length and energy spread is same between the two cases, where $\sigma_{z,\mathrm{SR}}$ and $\sigma_{p,\mathrm{SR}}$ are tuned in latter case.

Landau damping effect. The safe area squeezing due to the longitudinal wakefields certainly deserves further deeper studies possibly supported by analytical estimates and evaluations.

D. Bootstrapping injection

The bootstrapping injection [52] is a must for the future storage ring colliders because of the new X-Z coherent instability and the 3D flip-flop phenomenon [22]. The filling of the two beams in the machine is interleaved, and the imbalance of the charges of both beams is kept within a certain relative difference. We have performed a numerical scan of the horizontal tune for different bunch intensities thus simulating the injection process. In order to simplify the procedure the colliding bunch currents are considered to be equal, and we initiate higher current collisions starting with the equilibrium macroparticles data obtained at lower current. In this case, the possible 3D flip-flop effect is ignored to a large extent. If the collision is not stable at some specific tune, we will use the equilibrium macroparticles data of nearest stable working point for higher current collision. The horizontal tune scan result is shown in Fig. 8 with and without wakefield. As it is shown, the shape of the stable region is strongly distorted by the longitudinal wake filed. The width of safe area at design bunch population ($N = 8 \times 10^{10}$) is respectively 0.002 and 0.004 with and without wakefield. The stable region shifts with the increase of bunch population due to the change of incoherent synchrotron tune, while it remains fixed without wakefield.

IV. SUMMARY

In the conventional case, the longitudinal dynamics is nearly not affected by beam-beam interaction. However it is totally different in future e^+e^- storage ring colliders, such as CEPC/FCC-ee, where the bunch will be lengthened by the beamstrahlung effect in collision. Another important aspect for future lepton colliders is that there may exist head-tail like horizontal-synchrotron(X-Z) coherent instability in the case of large Piwinski angle collision. That is to say the horizontal oscillation will be affected by the longitudinal dynamics due to the beam-beam force. The blowup of horizontal beam size will change the beam-beam interaction and the corresponding beamstrahlung effect. Since the longitudinal wakefield would distort the longitudinal oscillation, it is self-consistent to directly consider the longitudinal wake force in the beam-beam simulation. The separate and combined effect of beamstrahlung and longitudinal beam coupling impedance at the Z factory is studied by simulation for CEPC case.

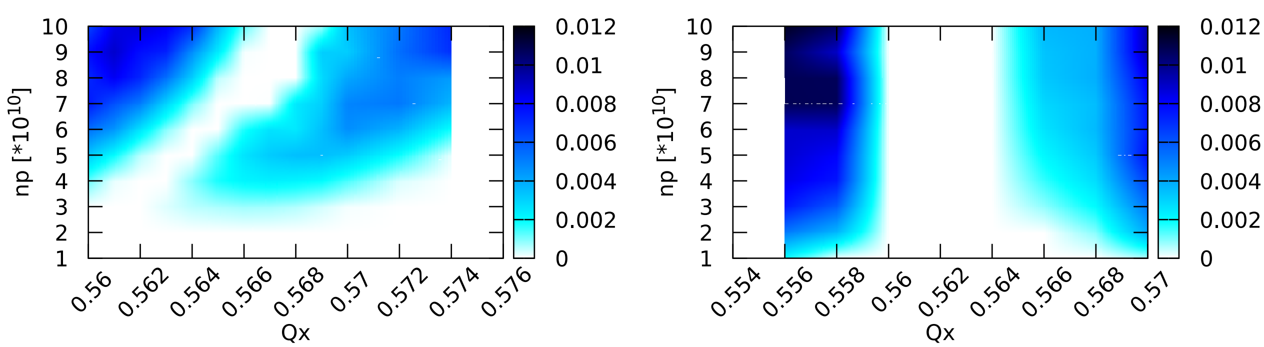

FIG. 8. Growth rate of horizontal beam size during bootstrapping injection for different tune. The left/right figure is for the case with and without impedance respectively.

The simulation study shows that the beamstrahlung effect strengthens the X-Z instability by squeezing the width of stable working point area about the value of horizontal beam-beam parameter. The distance between left bound of one stable region and the nearest resonance line $\nu_x = 0.5 + n\nu_s$ is about ξ_x, which is not sensitive to the beamstrahlung effect. This is different for the right bound, which shifts toward the left by about ξ_x comparing to that without beamstrahlung effect. To ensure that the width of stable tune area is as large as ξ_x, Q_s/ξ_x should be larger than 3 considering the beamstrahlung effect.

It is clearly found that the potential well effect of the longitudinal impedance may induce a safe area shift of tune space in collision due to the incoherent synchrotron tune shift. The larger tune spread helps to reduce the growth rate of the X-Z instability presumably due to the Landau damping effect. The reduction of stable working point space deserves further deeper studies possibly by analytical estimates.

The interplay of beamstrahlung effect and longitudinal wakefield leads to some additional bunch lengthening and energy spread reduction compared to that which only considers beamstrahlung effect. With the help of beamstrahlung effect, the collision could even be implemented above the single bunch microwave instability threshold. But the stable area is very limited and not easily achievable for our example.

The self-consistent simulation including beamstrahlung and longitudinal impedance is important and a must to study the stability of collision in future e^+e^- storage ring colliders. Both the machine parameters and impedance budget should be optimized carefully. We do not consider the possible asymmetry of the two colliding bunches, where 3D flip-flop may be a concern. Different impedance in two rings will make the picture more complicated. The theory analysis is being developed to evaluate the stability of the influence coming from longitudinal impedance in the case of large Piwinski angle. A whole self-consistent simulation considering real lattice and wakefield will be future work.

ACKNOWLEDGMENTS

This work is supported by National Key Programme for S&T Research and Development, China (Grant No. 2016YFA0400400), National Natural Science Foundation of China (No. 11775238, No. 11775239) and Chinese Academy of Sciences Visiting Professorship for Senior International Scientists (Grant No. 2019VMA0034).

[1] B. Richter, Design considerations for high-energy electron-positron storage rings, SLAC Tech. Report No. SLAC-PUB-240, 1966.

[2] M. Zobov and F. Zimmermann, *Handbook of Accelerator Physics and Engineering*, 2nd ed. (World Scientific, Singapore, 2013) Chap. Collision schemes for ring colliders, pp. 387–391.

[3] K. Oide, KEKB B-factory, the luminosity frontier, Progr. Theor. Phys. **122**, 69 (2009).

[4] M. Zobov, New generation electron-positron factories, Phys. Part. Nucl. **42**, 782 (2011).

[5] C. Yu *et al.*, BEPCII Performance and Beam Dynamics Studies on Luminosity, in *Proceedings of the 7th International Particle Accelerator Conference, Busan, Korea, 2016* (JACoW, Geneva, 2016), p. TUYA01.

[6] K. Hirata, Analysis of Beam-Beam Interactions with a Large Crossing Angle, Phys. Rev. Lett. **74**, 2228 (1995).

[7] K. Takayama, J. Kishiro, M. Sakuda, Y. Shimosaki, and M. Wake, Superbunch Hadron Colliders, Phys. Rev. Lett. **88**, 144801 (2002).

[8] F. Ruggiero and F. Zimmermann, Luminosity optimization near the beam-beam limit by increasing bunch length or crossing angle, Phys. Rev. Accel. Beams **5**, 061001 (2002).

[9] P. Raimondi, D. N. Shatilov, and M. Zobov, Beam-beam issues for colliding schemes with large Piwinski angle and crabbed waist, arXiv:physics/0702033.

[10] P. Raimondi and M. Zobov, Tune shift in beam-beam collisions with a crossing angle, INFN-LNF Tech. Report No. DAFNE-TECHNICAL-NOTE-G-58, 2003.

[11] D. Pestrikov, Vertical synchrobetatron resonances due to beam-beam interaction with horizontal crossing, Nucl. Instrum. Methods Phys. Res., Sect. A **336**, 427 (1993).

[12] P. Raimondi, M. Zobov, and D. Shatilov, Suppression of beam-beam resonances in crab waist collisions, in *Proceedings of the 11th European Particle Accelerator Conference, Genoa, 2008* (EPS-AG, Genoa, Italy, 2008), p. WEPP045.

[13] D. Shatilov, E. Levichev, E. Simonov, and M. Zobov, Application of frequency map analysis to beam-beam effects study in crab waist collision scheme, Phys. Rev. Accel. Beams **14**, 014001 (2011).

[14] M. Zobov *et al.*, Test of Crab-Waist Collisions at DAFNE Phi Factory, Phys. Rev. Lett. **104**, 174801 (2010).

[15] KEK press release, Superkekb collider achieves the world's highest luminosity, https://www.kek.jp/en/newsroom/2020/06/26/1400/.

[16] A. Blondel and F. Zimmermann, A high luminosity e^+e^- collider in the LHC tunnel to study the Higgs boson, arXiv:1112.2518.

[17] M. Bicer *et al.* (TLEP Design Study Working Group), First Look at the Physics Case of TLEP, J. High Energy Phys. 01 (2014) 164.

[18] A. Abada *et al.* (FCC), FCC-ee: The lepton collider: Future Circular Collider conceptual design report volume 2, Eur. Phys. J. ST **228**, 261 (2019).

[19] CEPC Study Group, CEPC conceptual design report: Volume 1—Accelerator, arXiv:1809.00285.

[20] V. Telnov, Restriction on the Energy and Luminosity of e^+e^- Storage Rings due to Beamstrahlung, Phys. Rev. Lett. **110**, 114801 (2013).

[21] K. Ohmi, N. Kuroo, K. Oide, D. Zhou, and F. Zimmermann, Coherent Beam-Beam Instability in

Collisions with a Large Crossing Angle, Phys. Rev. Lett. **119**, 134801 (2017).
[22] D. Shatilov, FCC-ee Parameter Optimization, ICFA Beam Dyn. Newslett. **72**, 30 (2017).
[23] M. Migliorati, E. Belli, and M. Zobov, Impact of the resistive wall impedance on beam dynamics in the Future Circular e^+e^- Collider, Phys. Rev. Accel. Beams **21**, 041001 (2018).
[24] E. Belli, P. C. Pinto, G. Rumolo, A. Sapountzis, T. Sinkovits, M. Taborelli, B. Spataro, M. Zobov, G. Castorina, and M. Migliorati, Electron cloud buildup and impedance effects on beam dynamics in the Future Circular e^+e^- Collider and experimental characterization of thin TiZrV vacuum chamber coatings, Phys. Rev. Accel. Beams **21**, 111002 (2018).
[25] D. Leshenok, S. Nikitin, and M. Zobov, Model to study interplay between Beamstrahlung and coupling impedance in future lepton colliders, arXiv:2004.02553.
[26] Y. Zhang, K. Ohmi, and L.-M. Chen, Simulation study of beam-beam effects, Phys. Rev. Accel. Beams **8**, 074402 (2005).
[27] K. Hirata and F. Ruggiero, Treatment of radiation for multiparticle tracking in electron storage rings, Part. Accel. **28**, 137 (1990), https://inspirehep.net/literature/281835.
[28] K. Hirata, Coherent betatron oscillation modes due to beam-beam interaction, Nucl. Instrum. Methods Phys. Res., Sect. A **269**, 7 (1988).
[29] S. Peggs and R. Talman, Beam-beam luminosity limitation in electron-positron colliding rings, Phys. Rev. D **24**, 2379 (1981).
[30] A. Piwinski, Dependence of the Luminosity on Various Machine Parameters and Their Optimization at PETRA, IEEE Trans. Nucl. Sci. **30**, 2378 (1983).
[31] G. Jackson and R. Siemann, The luminosity performance of CESR, Nucl. Instrum. Methods Phys. Res., Sect. A **286**, 17 (1990).
[32] S. Krishnagopal and R. Siemann, Bunch-length effects in the beam-beam interaction, Phys. Rev. D **41**, 2312 (1990).
[33] T. Chen, J. Irwin, and R. Siemann, Simulation of the beam halo from the beam-beam interaction, Phys. Rev. E **49**, 2323 (1994).
[34] D. Shatilov, Beam-beam simulations at large amplitudes and lifetime determination, Part. Accel. **52**, 65 (1996).
[35] K. Ohmi, M. Tawada, Y. Cai, S. Kamada, K. Oide, and J. Qiang, Luminosity limit due to the beam-beam interactions with or without crossing angle, Phys. Rev. Accel. Beams **7**, 104401 (2004).
[36] J. Qiang, M. A. Furman, R. D. Ryne, W. Fischer, and K. Ohmi, Recent advances of strongstrong beambeam simulation, Nucl. Instrum. Methods Phys. Res., Sect. A **558**, 351 (2006).
[37] K. Ohmi, Strong-strong Simulation for Super B Factories, in *Proceedings of IPAC'10* (Kyoto, Japan, 2010), p. TUPEB013; Strong-strong Simulations for Super B Factories II, in *Proceedings of IPAC2011* (San Sebastián, Spain, 2011), p. THPZ008.
[38] K. Hirata, H. Moshammer, and F. Ruggiero, A Symplectic beam-beam interaction with energy change, Part. Accel. **40**, 205 (1993).
[39] K. Ohmi and F. Zimmermann, FCC-ee/CEPC Beam-beam Simulations with Beamstrahlung, in *5th International Particle Accelerator Conference* (JACoW, Dresden, Germany, 2014), p. THPRI004, https://doi.org/10.18429/JACoW-IPAC2014-THPRI004.
[40] L. Palumbo, V. Vaccaro, and M. Zobov, Wake fields and impedance, in Proceedings of CAS-CERN Accelerator School: 5th Advanced Accelerator Physics Course (Rhodes, Greece, 1993), pp. 331–390, arXiv:physics/0309023.
[41] B. Zotter, Handbook of accelerator physics and engineering (World Scientific, Hackensack, USA, 2013), pp. 145–147.
[42] Y. Zhang, Beam-beam effects in BEPCII, in *ICFA Mini-Workshop on Beam-Beam Effects in Hadron Colliders* (CERN, Geneva, Switzerland, 2013), pp. 37–41, https://doi.org/10.5170/CERN-2014-004.37.
[43] K. Ohmi, Simulation of beam-beam effects in a circular e^+e^- collider, Phys. Rev. E **62**, 7287 (2000).
[44] K. Ohmi (private communication).
[45] ELEGANT, https://ops.aps.anl.gov/elegant.html.
[46] M. Migliorati (private communication).
[47] N. Wang, H. Zheng, D. Wang, Y. Wang, Q. Qin, W. Chou, D. Zhou, and K. Ohmi, Impedance and Collective Effects Studies in CEPC, in *Proceedings of the 55th ICFA Advanced Beam Dynamics Workshop on High Luminosity Circular e^+e^- Colliders Higgs Factory*, edited by N. Zhao and V. Schaa (JACOW, Beijing, China, 2014), p. 218; N. Wang, Y. Zhang, Y. Liu, S. Tian, K. Ohmi, and C. Lin, Mitigation of coherent beam instabilities in CEPC, presented at *ICFA mini-Workshop on MCBI, Zermatt, Switzerland, Sep. 2019*.
[48] CST STUDIO SUITE, http://www.cst.com.
[49] Y. H. Chin, ABCI User's Guide, KEK Report No. 2005-06, 2005, https://lib-extopc.kek.jp/preprints/PDF/2005/0524/0524006.pdf.
[50] N. Wang and Q. Qin, Resistive-wall impedance of two-layer tube, Phys. Rev. Accel. Beams **10**, 111003 (2007).
[51] A. Bogomyagkov, E. Levichev, and D. Shatilov, Beam-beam effects investigation and parameters optimization for a circular e^+e^- collider at very high energies, Phys. Rev. Accel. Beams **17**, 041004 (2014).
[52] S. Ogur, K. Oide, Y. Papaphilippou, D. Shatilov, and F. Zimmermann, Bunch schedules for the FCC-ee pre-injector (2018) https://doi.org/10.18429/JACoW-IPAC2018-MOPMF001.